IRIS AperTO

UNIVERSITÀ DEGLI STUDI DI TORINO

This is the author's final version of the contribution published as:

Francesca Bersani; Lingua, Marcello Francesco; Morena, Deborah; Foglizzo, Valentina; Miretti, Silvia; Lanzetti, Letizia; Carrà, Giovanna; Morotti, Alessandro; Ala, Ugo; Provero, Paolo; Chiarle, Roberto; Singer, Samuel; Ladanyi, Marc; Tuschl, Thomas; Ponzetto, Carola; and Riccardo Taulli. Deep Sequencing Reveals a Novel miR-22 Regulatory Network with Therapeutic Potential in Rhabdomyosarcoma. CANCER RESEARCH. 76 (20) pp: 6095-6106.
DOI: 10.1158/0008-5472.CAN-16-0709

The publisher's version is available at:
http://cancerres.aacrjournals.org/cgi/doi/10.1158/0008-5472.CAN-16-0709

When citing, please refer to the published version.

Link to this full text:
http://hdl.handle.net/

This full text was downloaded from iris - AperTO: https://iris.unito.it/

iris - AperTO

University of Turin's Institutional Research Information System and Open Access Institutional Repository

Deep sequencing reveals a novel miR-22 regulatory network with therapeutic potential in rhabdomyosarcoma

Francesca Bersani[§,1,2], Marcello Francesco Lingua[§,1,2], Deborah Morena[1,2], Valentina Foglizzo[1,2], Silvia Miretti[3], Letizia Lanzetti[1,4], Giovanna Carrà[5], Alessandro Morotti[5], Ugo Ala[6], Paolo Provero[6], Roberto Chiarle[2,6,7], Samuel Singer[8], Marc Ladanyi[9], Thomas Tuschl[10], Carola Ponzetto[1,2] and Riccardo Taulli[1,2]

[1] Department of Oncology, University of Turin, Orbassano, Turin, Italy

[2] CeRMS, Center for Experimental Research and Medical Studies, Turin, Italy

[3] Department of Veterinary Science, University of Turin, Grugliasco, Italy

[4] Candiolo Cancer Institute, Candiolo, Turin, Italy.

[5] Department of Clinical and Biological Sciences, University of Turin, Orbassano, Italy

[6] Department of Molecular Biotechnology and Health Sciences, University of Turin, Turin, Italy

[7] Department of Pathology, Boston Children's Hospital and Harvard Medical School, Boston, USA

[8] Department of Surgery, Memorial Sloan Kettering Cancer Center, New York, USA

[9] Department of Pathology, Memorial Sloan Kettering Cancer Center, New York, USA

[10] Department of RNA Molecular Biology, Howard Hughes Medical Institute, The Rockefeller University, New York, USA

Current address for V. Foglizzo: The Francis Crick Institute, Mill Hill Laboratory, The Ridgeway, London, UK

[§] These authors contributed equally to this work.

Running Title: mir-22 oncosuppressor network in Rhabdomyosarcoma.

Keywords: Rhabdomyosarcoma; miRNA deep sequencing; novel therapeutic strategies; oncosuppressor miRNAs; resistance to targeted therapy.

Note: Supplementary data for this article are available at Cancer Research Online (http://cancerres.aacrjournals.org/).

Grant support

This work was supported by the Italian Association for Cancer Research (AIRC Project number IG12089, C. Ponzetto; AIRC Start-up Project number 15405, R. Taulli; AIRC Project number IG15180, L. Lanzetti), EMBO Short Term Fellowship (ASTF No. 336-07, F. Bersani) and Regione Piemonte (IMMONC Project, C. Ponzetto).

Corresponding authors

R. Taulli and C. Ponzetto, Department of Oncology, University of Turin, Corso Massimo d'Azeglio 52, Turin 10126, Italy. e-mail: riccardo.taulli@unito.it; carola.ponzetto@unito.it; Phone: +39 011 633 4566; Fax: +39 011 633 6887.

Disclosure of Potential Conflicts of Interest

No potential conflicts of interest were disclosed.

Abstract word count: 209

Word count: 5460

Total number of figures: 7

Total number of references: 50

Abstract

Current therapeutic options for the pediatric cancer rhabdomyosarcoma (RMS) have not improved significantly, especially for metastatic RMS. In the present work, we performed a deep microRNA profiling of the three major human RMS subtypes, along with cell lines and normal muscle, to identify novel molecular circuits with therapeutic potential. The signature we determined could discriminate RMS from muscle, revealing a subset of muscle-enriched microRNA (myomiR), including miR-22 which was strongly underexpressed in tumors. miR-22 was physiologically induced during normal myogenic differentiation and was transcriptionally regulated by MyoD, confirming its identity as a myomiR. Once introduced into RMS cells, miR-22 decreased cell proliferation, anchorage-independent growth, invasiveness and promoted apoptosis. Moreover, restoring miR-22 expression blocked tumor growth and prevented tumor dissemination *in vivo*. Gene expression profiling analysis of miR-22-expressing cells suggested *TACC1* and *RAB5B* as possible direct miR-22 targets. Accordingly, loss and gain of function experiments defined the biological relevance of these genes in RMS pathogenesis. Finally, we demonstrated the ability of miR-22 to intercept and overcome the intrinsic resistance to MEK inhibition based on ERBB3 upregulation. Overall our results identified a novel miR-22 regulatory network with critical therapeutic implications in RMS.

Introduction

MicroRNAs (miRNAs) are small non-coding RNA molecules that regulate gene expression at the post-transcriptional level (1,2). In the last decade, the critical role of miRNAs has been reported in a wide range of biological functions including cell proliferation, migration, apoptosis, lineage commitment and differentiation (3,4). Thus it is not surprising that miRNAs are frequently dysregulated in cancer, where they can act either as oncogenes or oncosuppressors depending on their downstream target genes (5). Furthermore, miRNA signatures have been successfully used to classify human cancers and to discover novel attractive targets for therapeutic intervention (6).

Rhabdomyosarcoma (RMS) is the most common soft tissue sarcoma of childhood and the third one in young adults (7). Histopathological classification includes three major subtypes: embryonal (ERMS), alveolar (ARMS) and pleomorphic (PRMS). ERMS are more frequent, genetically heterogeneous and associated with a better prognosis (8–10). Conversely ARMS are less common and more aggressive, with a worse outcome. A dismal clinical prognosis is genetically ascribed to the PAX3/7-FKHR translocation present in more than 80% of cases (11). Notably, RMS cells are positive for myogenic markers and resemble normal muscle progenitors but are unable to complete the differentiation program (12). We have previously showed that the muscle-enriched miRNAs miR-1 and miR-206 (myomiRs) reprogram the RMS expression profile toward that of a normal muscle, in a process involving the post-transcriptional regulation of hundreds of genes, among which *MET*, *G6PD*, *ACTL6A* and *SMYD1* (13–15).

In this work we used a next-generation miRNA sequencing approach (NGS) on a large panel of human RMS primary tumors, including the three major subtypes, cell lines and normal muscle tissues, to identify novel miRNA regulatory circuits involved in RMS pathogenesis. The miRNA signature clearly distinguished malignant tissues from normal skeletal muscle and revealed a strong reduction of miR-22 and miR-378 in RMS. However, only the rescue of miR-22 exerted a very potent oncosuppressor function, interfering with the transformed properties of RMS cells both *in vitro* and *in vivo*. Gene expression profiling of miR-22-expressing RMS cells suggested *TACC1* and *RAB5B* as two critical miR-22 targets, while *ERBB3* emerged only upon treatment of mutant NRAS-positive cells with MEK inhibitors. Altogether our NGS miRNA sequencing effort uncovered a novel miR-22 oncosuppressor regulatory circuit that opposes RMS tumor growth and interferes with the resistance to MEK inhibition.

Materials and Methods

Cell lines

Embryonal (RD18, CCA, HTB82, TE671, indicated as Myosarcoma_TE) and alveolar (RH4, RH30) RMS cell lines were provided by Dr. Pier-Luigi Lollini (University of Bologna, Bologna, Italy). The pleomorphic cell line RMS-559 was obtained from Samuel Singer's lab. HTB82 and TE671 cell lines were originally obtained from ATCC (Manassas, VA, USA); RH30 and RH4 (RH41) were originally obtained from DSMZ (Braunschweig, Germany); CCA and RD18 cell lines were originally stabilized in Pier-Luigi Lollini's lab. C2C12 myoblasts were originally obtained from DSMZ (Braunschweig, Germany). Satellite cells, RD18 NpBI-206 cells, RD18 NpBI-206AS cells and NIH 10T½ NpBI-MyoD cells were previously described (13–15). RMS cell lines, NIH 10T½ cells, satellite cells and myoblasts were grown as previously described (13). RD18, HTB82, TE671, RH4 and RH30 cell lines were routinely authenticated (every six months) by short tandem repeat (STR) analysis. CCA cell line, for which STR profile is unknown, was authenticated by sequencing of the KRAS Q61L mutation.

Patients

Primary human tumors of embryonal, alveolar and pleomorphic histology (or their RNA) and muscle tissues were obtained from Memorial Sloan Kettering Cancer Center, New York, NY, USA, with informed consent prior to the inclusion in the study and with obscured identity, according to the recommendations of the Institutional Review Board of the Memorial Sloan Kettering Cancer Center. For all ARMS samples, the presence of the

specific fusion transcripts was confirmed by RT-PCR. Of the 14 RMS included in this study, 10 had previously been extensively analyzed by gene expression profiling, confirming subtype-specific signatures (16). Normal cell contamination of the processed specimens was reviewed and assessed to be less than 20%.

Small RNA isolation and library generation

RNA from cultured cells, freshly frozen and OCT-embedded tissues was extracted using Trizol (Invitrogen). RNA from formalin-fixed, paraffin-embedded tissues was isolated with MasterPure RNA Purification Kit (Epicentre Biotechnologies). Despite a different yield of total RNA, the miRNA expression profiles of all types of samples are well correlated across the various histological subtypes. cDNA libraries preparation was performed as previously described (17). A brief explanation can be found in Supplementary Materials and Methods. Sequencing was performed at Memorial Sloan Kettering Cancer Center and raw data are deposited on SRA platform, ID PRJNA326118. Computational analysis of the raw data was done in collaboration with Mihaela Zavolan's lab, University of Basel, Switzerland.

Lentiviral vectors and siRNAs

NpBI-22 and NpBI-378 vectors were generated as previously described (13). Vectors and si/shRNAs are detailed in Supplementary Materials and Methods.

Northern blot

Northern blot analysis was performed as previously described (13). ^{32}P-labeled DNA oligos are listed in Supplementary Materials and Methods.

Microarrays and data analysis

Affymetrix Human GeneChip Gene ST 1.0 arrays (Affymetrix) were hybridized at the Cogentech core facility (Milano, Italy) according to standard Affymetrix protocols. The array data were analyzed with the Partek Genomics Suite. All genes showing differential expression between the 2 experimental conditions found to be significant by ANOVA were then subjected to unsupervised hierarchical clustering. Microarray data were deposited under series GSE83805.

Sensor vector generation and reporter assays

GFP/luciferase reporter vectors were co-transfected with synthetic pre-miRNA (miRNA precursor hsa-miR-22, PM10203, ThermoFisher) in HEK 293T cells. For MyoD binding sites validation, luciferase reporter vectors were transfected in NIH 10T½ NpBI-MyoD cells. Detailed information is summarized in Supplementary Materials and Methods.

Real-time PCR analysis

Taq-Man miRNA Assays (Applied Biosystems) were used for relative quantification of mature miRNAs. MiR-16 was used to normalize the results. Gene expression was evaluated as previously described (15), using primers listed in Supplementary Materials and Methods. HuPO was used to normalize the results.

Cell proliferation assay, cell cycle analysis and assessment of apoptosis

For proliferation assay, cells were plated in 24-well plates at a density of 5×10^3 per well. Proliferation was evaluated by CellTiter-Glo (Promega) following the manufacturer's instructions. Cell cycle analysis and apoptosis were performed as previously described (13).

Anchorage-independent cell-growth, invasiveness and scratch wound assays

Soft-agar assay was performed as previously described (13). After 2 weeks or one month in culture colonies were counted and images were acquired at 5X magnification. Invasiveness was examined using a membrane invasion culture system (Corning Life Sciences) as previously described (13). Scratch wound assay is detailed in Supplementary Materials and Methods.

Western blot, FACS and immunohistochemistry

Western blot assay, MHC immunostaining for FACS analysis and immunohistochemistry were performed as previously described (13,15). All antibodies used are listed in Supplementary Materials and Methods.

Chromatin immunoprecipitation assay

ChIP assay was performed as previously described (18). Antibodies and primers are listed in Supplementary Materials and Methods.

Inhibitors

Selumetinib (AZD6244, Selleckchem) and Lapatinib (GW-572016, Selleckchem) were used at 1μM. DMSO was used as a control.

In vivo tumorigenesis assay

For *in vivo* tumor growth, cells were resuspended in sterile PBS and injected subcutaneously into the flank or in the tail vein of female *nu/nu* mice (Charles River Laboratories). Tumor size was measured as previously described (13). Conditional miR-22 expression was induced in mice by administration of 1 mg/ml of doxycycline in the drinking water. All animal procedures were approved by the Ethical Committee of the University of Turin and by the Italian Ministry of Health.

Statistical analysis

Two-tailed paired or unpaired Student‘s *t* test was used to evaluate statistical significance: $^{NS}P>0.05$; *P<0.05; **P<0.01; ***P<0.001. All mean values are expressed as SD or SEM, as specified in figure legends, and derive from at least three independent experiments.

Results

Small RNA cloning and deep sequencing reveal a distinct miRNA signature in RMS compared to normal muscle

To identify novel miRNAs involved in RMS pathogenesis, we profiled miRNA expression in 21 primary human RMS and 4 normal muscles by NGS of small RNA libraries. Unsupervised hierarchical clustering showed a strong distinction between muscles and tumors (Fig. 1A, Supplementary Fig. S1A and Supplementary Table S1), revealing a clear RMS-related miRNA signature and indicating a profound miRNA dysregulation in malignant tissues. However, miRNA profiling did not distinguish among ERMS, ARMS and PRMS, indicating that miRNAs cannot be predictive of specific subtypes. Notwithstanding, we identified few families overrepresented in tumor samples (including miR-130a and miR-335-5p; Fig. 1A), and not expressed in muscle. As expected, myomiRs (miR-1/206/133) were particularly underexpressed in RMS (Fig. 1A, Supplementary Fig. S1A and Supplementary Tables S1 and S2), confirming the good reliability of our signature.

Interestingly, in the top 5 muscle-enriched miRNAs we detected also miR-378 and miR-22 (Fig. 1A and Supplementary Table S2). While miR-378 has been recently associated to RMS pathogenesis (19), the role of miR-22 has remained so far unexplored.

miR-22 and -378 are muscle-enriched miRNAs

We first validated miR-22 and miR-378 expression levels using alternative approaches. Northern blot analysis confirmed the enrichment of miR-22 and miR-378 in

normal muscle, while both were barely detectable in primary RMS (Fig. 1B). Furthermore, we assessed their presence and induction in different myogenic systems: differentiated satellite cells and C2C12 myoblasts, miR-206-expressing RMS cells (13) and MyoD-reprogrammed 10T½ fibroblasts (15). In all models used and as previously reported for miR-22 in C2C12 myoblasts (20), miR-22 and -378 were strongly induced during differentiation (Fig. 1C-F), suggesting the involvement of both miRNAs in the myogenic program. Notably, for both miRNAs there is complete homology in the mature sequence of human and mouse, suggesting conserved functions. Interestingly, we did not observe any substantial difference of expression between the two miRNAs in differentiated satellite cells and myoblasts. However, miR-378 was the most upregulated miRNA in MyoD-reprogrammed 10T½ fibroblasts, whereas miR-22 was particularly induced in miR-206-expressing RMS cells. Thereby, both miRNAs are involved in the myogenic program but miR-22 may exert a critical role in RMS.

miR-22 acts as a potent oncosuppressor by interfering with the transformed properties of RMS cells

To investigate the role of the two newly identified muscle-enriched miRNAs in RMS pathogenesis, we generated RMS cells that conditionally expressed miR-22 or -378 in a Doxycycline (Dox) -dependent manner. The system was tightly Dox-regulated with no expression in normal medium, while Dox administration resulted in a robust miRNA induction comparable to that observed in mouse skeletal muscle, especially for miR-22 (Supplementary Fig. S2A and B). MiR-22 induction arrested proliferation of both ERMS (RD18) and ARMS (RH30) cells (Fig. 2A and B). Accordingly, cell cycle distribution

analysis showed a reduction in the S phase and a concomitant accumulation in the G0/G1 and in G2/M phases of the cell cycle (Fig. 2C and D). Furthermore, miR-22 promoted apoptosis both in ERMS and ARMS cells (Fig. 2E and F). These two aspects were confirmed by changes in expression of proteins involved in cell proliferation and apoptosis (Fig. 2G). We next investigated the ability of miR-22 to interfere with the transformed properties of RMS cells. Long-term miR-22 induction significantly impaired anchorage-independent growth in soft-agar (Fig. 2H and I). Moreover, miR-22 expression impaired invasiveness in matrigel assays (Fig. 2J and K).

Interestingly, miR-22 is hosted in the second exon of a long non-coding RNA (lncRNA, MIR22HG). Thus, to rule out the possibility that part of the oncosuppressor potential observed was associated to the lncRNA, we generated a vector expressing the same miR-22 precursor, but with the miR-22 seed sequence completely mutagenized. Using this construct, we did not observe mature miR-22 production nor an effect on RMS cell proliferation (Supplementary Fig. S2C and D). Finally, we also explored the oncosuppressor potential of miR-378. Differently from miR-22, miR-378 was, in our setting, less effective in interfering with the transformed features of RMS cells (Supplementary Fig. S2E-G and data not shown). Thus, we decided to further investigate the biological relevance of miR-22 only.

MyoD binds to the promoter region of miR-22 at the onset of myogenic differentiation and activates its transcription

The observation that miR-22 was upregulated during myogenic cell differentiation suggested that muscle regulatory factors might be responsible for its activation. MyoD is

the master transcription factor that governs the myogenic program (21). We therefore examined the core promoter of miR-22, consisting of 1200 bp and we identified four predicted MyoD recognition sites, conserved in the mouse and human genes (Fig. 3A, black boxes). Thus we set up a ChIP assay on MyoD-reprogrammed 10T½ fibroblasts. As expected, MyoD and acetyl-histone H3 binding at the miR-22 core promoter regions was observed only upon MyoD induction (Fig. 3B and C). To verify whether MyoD binding resulted in transcriptional activity, we generated three sensor constructs (sensor 22.0, 22.1 and 22.2) containing 419, 586 and 1089 bp upstream of pre-miR-22 fused to a luciferase reporter. Upon MyoD induction, only sensors 22.1 and 22.2, containing two and four putative MyoD binding sites respectively, displayed strong transcriptional activity (Fig. 3D). Notwithstanding, no significant difference in luciferase induction was observed between the 22.1 and 22.2 constructs, indicating that the first two putative sites, located on the 22.1 fragment, were mainly responsible for MyoD binding. Accordingly, mutation of both E-boxes (I+II) of the 22.1 construct completely abolished luciferase induction (Fig. 3D), indicating that these two regulatory elements are essential for MyoD transcriptional activity.

We previously showed that miR-206, another MyoD-transcriptionally regulated myomiR (22), is able to force RMS cells to resume differentiation (13). However, when we explored the myogenic potential of miR-22, we did not observe any sign of terminal RMS differentiation (Supplementary Fig. S3A and B). Considering that MyoD promotes myogenic differentiation by first arresting myoblast proliferation and subsequently by driving terminal differentiation, it is likely that miR-22 is involved only in the MyoD-dependent cell cycle arrest.

miR-22 abrogates tumor growth and dissemination

The ability of miR-22 to act as a potent oncosuppressor encouraged us to explore its therapeutic potential *in vivo*. We first assessed whether miR-22 was sufficient to prevent tumor growth. To this aim, engineered RMS cells were injected into immunocompromised mice that were immediately treated with doxycycline. While in control mice tumors grew rapidly, miR-22 induction completely abolished RMS formation (Fig. 4A). Then we evaluated the therapeutic potential of miR-22 by inducing the miRNA only after the tumor became palpable. Also in this case miR-22 expression resulted in potent inhibition of RMS growth (Fig. 4B). The anti-tumorigenic effect of miR-22 was confirmed by reduction of Ki67 staining and by the presence of cleaved Caspase-3-positive cells in treated mice (Fig. 4C). Lastly, we tested miR-22 ability to interfere with RMS cell dissemination. Tail vein injection of non-induced cells resulted in their rapid dissemination in lungs and kidneys (Fig. 4D and E, NI). Conversely, miR-22 induction fully inhibited macro and micro metastasis formation in both organs (Fig. 4D and E, IND). Immunohistochemistry analysis confirmed the presence of actively proliferating tumor cells only in tissues obtained from control mice (Fig. 4D and E).

Gene expression profiling of miR-22-expressing RMS cells identifies TACC1 and RAB5B as two critical targets

To investigate the mechanism by which miR-22 interfered with the transformed properties of RMS cells, we compared gene expression profiling of RD18 NpBI-22 induced (IND) cells with non-induced (NI) cells. Unsupervised hierarchical clustering

resulted in a dendrogram with two clearly distinct branches separating miR-22-expressing cells from controls (Supplementary Fig. 4A). In particular, ANOVA analysis revealed a total of 494 significantly modulated transcripts, among which 263 were downregulated in the induced condition. To identify possible miR-22 target genes we analyzed the downmodulated transcripts using the EIMMo miRNA target prediction server (Supplementary Table S3). Among them, *Transforming Acidic Coiled-Coil Containing Protein 1* (*TACC1*) and *RAB5B* resulted of particular interest. *TACC1* is indeed a cancer-related gene located on chromosome 8p11, amplified in breast cancer (23) and translocated in glioblastoma (24). RAB5, instead, is a small GTPase involved in intracellular trafficking and migration (25). Notably, *TACC1* 3'UTR contains two miR-22 MREs, while *RAB5B* 3'UTR includes three of them (Supplementary Fig. 4D), suggesting that both genes could be directly and efficiently downmodulated by miR-22. Western blot analysis confirmed a strong TACC1 and RAB5B downregulation upon miR-22 induction, both *in vitro* and *in vivo* (Supplementary Fig. 4B and C). Moreover, sensor vectors expressing the mutagenized or the wild type miR-22 MREs of *TACC1* and *RAB5B* 3'UTRs showed that both genes were indeed miR-22 direct targets (Supplementary Fig. 4E and F).

TACC1 and RAB5B control the transformed properties of RMS cells

To study the functional relevance of TACC1 in RMS pathogenesis, we first tested the effects of its downregulation in RMS cells. Interestingly, TACC1 silencing (Fig. 5A) impaired cell proliferation (Fig. 5B, C and F), promoted apoptosis (Fig. 5D and F) and inhibited soft-agar growth of both ERMS and ARMS cells (Fig. 5E). Conversely, TACC1

overexpression (Fig. 5G) partially rescued the anchorage-independent growth ability of miR-22-expressing RMS cells (Fig. 5H).

RAB5 expression has been previously linked with tumor cell migration and invasion (26,27). However, RAB5 is encoded by three distinct paralogs: *RAB5A*, *RAB5B* and *RAB5C*. Interestingly, *RAB5B* is the prevalent isoform expressed in cells of both RMS subtypes (Fig. 6A and B). Thus, we silenced RAB5B in RMS cells (Fig. 6C) and explored whether RAB5B was involved in RMS cell motility. Wound healing assay showed that RAB5B silencing delayed wound closure at the evaluated time point (Fig. 6D and E), whereas RAB5B overexpression (Fig. 6F) enhanced migration towards the wounded area of miR-22-expressing RMS cells (Fig. 6G and H). Altogether, our data support a model in which the oncosuppressor role of miR-22 in RMS cells is at least in part due to TACC1 and RAB5B downregulation.

miR-22 prevents intrinsic resistance to MEK inhibition by intercepting ERBB3 upregulation

Comprehensive genomic analyses revealed that the RAS pathway is frequently mutated in ERMS tumors (8–10). Although the pharmacological inhibition of constitutively active RAS proteins remains challenging (28), small molecule inhibitors directed against the downstream ERK signalling offer an alternative RAS pathway-targeted strategy. Nevertheless, the efficacy of MEK inhibitors in cancer patients is modest (29). This partial response has been frequently associated to the activation of compensatory feedback pathways involved in primary resistance (30,31). Notably, RD18 cells harbour the constitutive active form of NRAS [NRAS Q61H (32)] and are relatively

resistant to MEK inhibition (30) (Fig. 7A). Considering the strong oncosuppressor potential of miR-22, we explored whether this miRNA could also play a role in preventing resistance to the MEK inhibitor Selumetinib. Intriguingly, miR-22 induction in combination with MEK inhibition potently blocked RD18 cell growth, enhancing the effects of the single treatment alone (Fig. 7A and C). Interestingly, a recent synthetic lethal screening approach revealed that a common mechanism of primary resistance to MEK inhibitors implicates ERBB3 upregulation (33). Also in RD18 cells, Selumetinib treatment resulted in a strong ERBB3 induction (Fig. 7B). Conversely, in the presence of miR-22, Selumetinib was unable to upregulate ERBB3 (Fig. 7B), suggesting that miR-22 was interfering with ERBB3 expression. Accordingly, *ERBB3* transcript contains a functional miR-22 MRE in the 3'UTR (Fig. 7D) and thus miR-22 can immediately intercept ERBB3 expression upon Selumetinib treatment. Finally, the combination treatment based on Selumetinib plus Lapatinib also enhanced Selumetinib-mediated soft-agar growth inhibition (Fig. 7C), further confirming the functional relevance of ERBB3 pathway activation in driving MEK inhibitor resistance.

Discussion

In this work we performed miRNA NGS on primary RMS samples, RMS cell lines and normal skeletal muscles. The miRNA signature revealed a clear distinction between muscle and tumor specimens but, in contrast to a previous study (34), we were unable to distinguish the three histological categories included in our samples (ERMS, ARMS and PRMS), suggesting a common alteration in miRNA expression profile independently on RMS subtype.

However, our miRNA expression profiling revealed that miR-378 and miR-22, together with other previously characterized myomiRs, were markedly underrepresented in RMS compared to normal muscle tissue. While miR-378 downregulation in RMS has been recently reported (19), the role of miR-22 has remained so far unexplored. The biological significance of miR-22 in cancer is still controversial and seems to be context specific. While it is generally considered as oncosuppressor (35–38), two recent papers support its oncogenic potential (39,40). Although miR-22 is ubiquitously expressed, it is particularly enriched in cardiac muscle, where it is involved in cardiac hypertrophy and remodelling (41,42). According to our data, miR-22 is also abundant in skeletal muscle and the muscle-specific transcription factor MyoD plays a critical role in regulating its expression in myogenic cells. While genome-wide analysis of MyoD binding regions in C2C12 myoblasts indicated its presence in the promoter of four miRNAs, including miR-22 (21), here we identified the two paired sites upstream of miR-22, critical for both MyoD binding and transcription. As reported by others (43), MyoD is not functional in RMS despite its ability to associate with coactivators and to bind to DNA, and this could

explain why miR-22 expression is impaired in this tumor type. MyoD acts at two levels in myogenesis regulating first the block of cell proliferation and then muscle-specific gene expression (44). The mediators of the former effect are still poorly understood. Our data suggest that the anti-proliferative action of MyoD is accomplished, at least in part, post-transcriptionally by miR-22. Indeed, when ectopically expressed in RMS cells of both embryonal and alveolar histology, miR-22 showed a prominent oncosuppressor potential by impairing cell proliferation, invasiveness and significantly increasing apoptosis. Besides its strong *in vitro* effect, miR-22 also displayed a remarkable anti-tumor effect *in vivo*, leading to a significant reduction of RMS growth and metastatic potential.

By gene expression analysis in miR-22-expressing RD18 cells we identified TACC1 and RAB5B as promising miR-22-regulated candidates. TACC1 and RAB5, both acting on cytoskeleton dynamic, have been previously shown to be involved in cell transformation and in tumor dissemination. *TACC1* was first identified as the sole coding sequence within the 8p11 breast cancer-associated amplicon and capable of transforming mouse fibroblasts by itself (23). Interestingly, a significant percentage of ERMS (up to 92%) displays gain of the entire chromosome 8 (8–11), suggesting a possible oncogenic role for genes harboured in this chromosome. Conversely, RAB5 family members are critical trafficking molecules that directly influence several aspects of cell migration (26,27). Accordingly, modulation of either target genes influenced the transformed properties of RMS cells. While TACC1 was mainly involved in the regulation of RMS cell growth, RAB5B prevalently controlled RMS cell motility. Interestingly, *RAB5A* is also a predicted target of miR-206, and considering that all RAB5 members play a redundant role in actin cytoskeleton dynamic, we cannot rule out the possibility that more

complex circuits involving myomiRs and RAB5 genes are dysregulated in RMS pathogenesis.

Since a single miRNA can potentially regulate hundreds of different transcripts, other targets are likely to contribute to miR-22 therapeutic efficacy. This concept is particularly relevant considering the widely accepted view that cancer is a Darwinian disease (31). Regrettably, the targeted therapy approach, less toxic than conventional chemotherapy, often gives rise to adaptive responses that result in resistance (31). In this context, a combination of a target therapy with a pleotropic miRNA with therapeutic potential could be beneficial in preventing mechanisms of resistance. We thus explored the functional relevance of miR-22 action in this setting. Interestingly, RD18 cells that harbor a constitutive active form of NRAS are modestly responsive to Selumetinib treatment and here we have shown that this is in part related to a feedback mechanism of compensation based on ERBB3 upregulation. Notably, *ERBB3* was not present in our list of downregulated genes upon miR-22 induction, although it includes one functional MRE. This apparent discrepancy is based on the fact the profiling was performed in cells growing in medium without drugs. Indeed, ERBB3 upregulation was observed only upon Selumetinib treatment, and in this condition, the concomitant presence of miR-22 efficiently interfered with the mechanism of resistance. Accordingly, we have shown that the combination of drugs (Selumetinib + Lapatinib) was more effective than single treatments. However this pharmacological strategy could still be inadequate to prevent the emergence of further resistance, especially in highly heterogeneous ERMS.

For this reasons, future therapeutic strategies against RMS could take advantage of using pleotropic oncosuppressor miRNAs (13,19,45–50), among which we now propose miR-22.

Overall, our miRNA NGS and profiling reveal a novel miRNA network in which miR-22 plays a critical role by acting at multiple levels of regulation. Although drugs directed against individual miR-22 targets may provide useful alternative strategies in RMS, our data suggest that, once the problem of miRNA delivery will be overcome, miR-22 could represent an effective therapeutic option alone or in combination with targeted agents in primary tumors, distant metastases and to prevent drug-induced primary resistance.

Acknowledgments

The authors wish to thank Pavel Morozov (Rockefeller University, New York, NY) for bioinformatic support and Maria Stella Scalzo (University of Turin) for help with immunohistochemical analysis. The support of the Fondazione Ricerca Molinette Onlus is gratefully acknowledged.

References

1. Bartel DP. MicroRNAs: target recognition and regulatory functions. Cell. 2009;136(2):215–33.

2. Fabian MR, Sonenberg N, Filipowicz W. Regulation of mRNA translation and stability by microRNAs. Annu Rev Biochem. 2010;79:351–79.

3. Krol J, Loedige I, Filipowicz W. The widespread regulation of microRNA biogenesis, function and decay. Nat Rev Genet. 2010;11(9):597–610.

4. Cacchiarelli D, Martone J, Girardi E, Cesana M, Incitti T, Morlando M, et al. MicroRNAs Involved in Molecular Circuitries Relevant for the Duchenne Muscular Dystrophy Pathogenesis Are Controlled by the Dystrophin/nNOS Pathway. Cell Metab. 2010;12(4):341–51.

5. Nana-Sinkam SP, Croce CM. MicroRNA regulation of tumorigenesis, cancer progression and interpatient heterogeneity: towards clinical use. Genome Biol. 2014;15(9):445.

6. Hayes J, Peruzzi PP, Lawler S. MicroRNAs in cancer: biomarkers, functions and therapy. Trends Mol Med. 2014;20(8):460–9.

7. Shern JF, Yohe ME, Khan J. Pediatric Rhabdomyosarcoma. Crit Rev Oncog. 2015;20(3–4):227–43.

8. Chen X, Stewart E, Shelat AA, Qu C, Bahrami A, Hatley M, et al. Targeting oxidative stress in embryonal rhabdomyosarcoma. Cancer Cell. 2013;24(6):710–24.

9. Shern JF, Chen L, Chmielecki J, Wei JS, Patidar R, Rosenberg M, et al. Comprehensive genomic analysis of rhabdomyosarcoma reveals a landscape of alterations affecting a common genetic axis in fusion-positive and fusion-negative tumors. Cancer Discov. 2014;4(2):216–31.

10. Seki M, Nishimura R, Yoshida K, Shimamura T, Shiraishi Y, Sato Y, et al. Integrated genetic and epigenetic analysis defines novel molecular subgroups in rhabdomyosarcoma. Nat Commun. 2015;6:7557.

11. Williamson D, Missiaglia E, de Reyniès A, Pierron G, Thuille B, Palenzuela G, et al. Fusion gene-negative alveolar rhabdomyosarcoma is clinically and molecularly indistinguishable from embryonal rhabdomyosarcoma. J Clin Oncol. 2010;28(13):2151–8.

12. Keller C, Guttridge DC. Mechanisms of impaired differentiation in rhabdomyosarcoma. FEBS J. 2013;280(17):4323–34.

13. Taulli R, Bersani F, Foglizzo V, Linari A, Vigna E, Ladanyi M, et al. The muscle-specific microRNA miR-206 blocks human rhabdomyosarcoma growth in xenotransplanted mice by promoting myogenic differentiation. J Clin Invest. 2009;119(8):2366–78.

14. Taulli R, Foglizzo V, Morena D, Coda DM, Ala U, Bersani F, et al. Failure to downregulate the BAF53a subunit of the SWI/SNF chromatin remodeling complex

contributes to the differentiation block in rhabdomyosarcoma. Oncogene. 2014;33(18):2354–62.

15. Coda DM, Lingua MF, Morena D, Foglizzo V, Bersani F, Ala U, et al. SMYD1 and G6PD modulation are critical events for miR-206-mediated differentiation of rhabdomyosarcoma. Cell Cycle. 2015;14(9):1389–402.

16. Laé M, Ahn EH, Mercado GE, Chuai S, Edgar M, Pawel BR, et al. Global gene expression profiling of PAX-FKHR fusion-positive alveolar and PAX-FKHR fusion-negative embryonal rhabdomyosarcomas. J Pathol. 2007;212(2):143–51.

17. Hafner M, Landgraf P, Ludwig J, Rice A, Ojo T, Lin C, et al. Identification of microRNAs and other small regulatory RNAs using cDNA library sequencing. Methods. 2008;44(1):3–12.

18. Palacios D, Mozzetta C, Consalvi S, Caretti G, Saccone V, Proserpio V, et al. TNF/p38α/polycomb signaling to Pax7 locus in satellite cells links inflammation to the epigenetic control of muscle regeneration. Cell Stem Cell. 2010;7(4):455–69.

19. Megiorni F, Cialfi S, McDowell HP, Felsani A, Camero S, Guffanti A, et al. Deep Sequencing the microRNA profile in rhabdomyosarcoma reveals down-regulation of miR-378 family members. BMC Cancer. 2014;14:880.

20. Marzi MJ, Puggioni EMR, Dall'Olio V, Bucci G, Bernard L, Bianchi F, et al. Differentiation-associated microRNAs antagonize the Rb-E2F pathway to restrict proliferation. J Cell Biol. 2012;199(1):77–95.

21. Cao Y, Kumar RM, Penn BH, Berkes CA, Kooperberg C, Boyer LA, et al. Global and gene-specific analyses show distinct roles for Myod and Myog at a common set of promoters. EMBO J. 2006;25(3):502–11.

22. Rao PK, Kumar RM, Farkhondeh M, Baskerville S, Lodish HF. Myogenic factors that regulate expression of muscle-specific microRNAs. Proc Natl Acad Sci U S A. 2006;103(23):8721–6.

23. Still IH, Hamilton M, Vince P, Wolfman A, Cowell JK. Cloning of TACC1, an embryonically expressed, potentially transforming coiled coil containing gene, from the 8p11 breast cancer amplicon. Oncogene. 1999;18(27):4032–8.

24. Singh D, Chan JM, Zoppoli P, Niola F, Sullivan R, Castano A, et al. Transforming fusions of FGFR and TACC genes in human glioblastoma. Science. 2012;337(6099):1231–5.

25. Lanzetti L, Palamidessi A, Areces L, Scita G, Di Fiore PP. Rab5 is a signalling GTPase involved in actin remodelling by receptor tyrosine kinases. Nature. 2004;429(6989):309–14.

26. Palamidessi A, Frittoli E, Garré M, Faretta M, Mione M, Testa I, et al. Endocytic trafficking of Rac is required for the spatial restriction of signaling in cell migration. Cell. 2008;134(1):135–47.

27. Liu S, Chen X, Zheng H, Shi S, Li Y. Knockdown of Rab5a expression decreases cancer cell motility and invasion through integrin-mediated signaling pathway. J Biomed Sci. 2011;18:58.

28. Patricelli MP, Janes MR, Li L-S, Hansen R, Peters U, Kessler LV, et al. Selective Inhibition of Oncogenic KRAS Output with Small Molecules Targeting the Inactive State. Cancer Discov. 2016 Jan 6;doi: 10.1158/2159-8290.CD-15-1105.

29. Samatar AA, Poulikakos PI. Targeting RAS-ERK signalling in cancer: promises and challenges. Nat Rev Drug Discov. 2014;13(12):928–42.

30. Renshaw J, Taylor KR, Bishop R, Valenti M, De Haven Brandon A, Gowan S, et al. Dual blockade of the PI3K/AKT/mTOR (AZD8055) and RAS/MEK/ERK (AZD6244) pathways synergistically inhibits rhabdomyosarcoma cell growth in vitro and in vivo. Clin Cancer Res. 2013;19(21):5940–51.

31. Misale S, Arena S, Lamba S, Siravegna G, Lallo A, Hobor S, et al. Blockade of EGFR and MEK intercepts heterogeneous mechanisms of acquired resistance to anti-EGFR therapies in colorectal cancer. Sci Transl Med. 2014;6(224):224ra26.

32. Chardin P, Yeramian P, Madaule P, Tavitian A. N-ras gene activation in the RD human rhabdomyosarcoma cell line. Int J Cancer. 1985;35(5):647–52.

33. Sun C, Hobor S, Bertotti A, Zecchin D, Huang S, Galimi F, et al. Intrinsic resistance to MEK inhibition in KRAS mutant lung and colon cancer through transcriptional induction of ERBB3. Cell Rep. 2014;7(1):86–93.

34. Subramanian S, Lui WO, Lee CH, Espinosa I, Nielsen TO, Heinrich MC, et al. MicroRNA expression signature of human sarcomas. Oncogene. 2008;27(14):2015–26.

35. Zhang J, Yang Y, Yang T, Liu Y, Li A, Fu S, et al. microRNA-22, downregulated in hepatocellular carcinoma and correlated with prognosis, suppresses cell proliferation and tumourigenicity. Br J Cancer. 2010;103(8):1215–20.

36. Xu D, Takeshita F, Hino Y, Fukunaga S, Kudo Y, Tamaki A, et al. miR-22 represses cancer progression by inducing cellular senescence. J Cell Biol. 2011;193(2):409–24.

37. Tsuchiya N, Izumiya M, Ogata-Kawata H, Okamoto K, Fujiwara Y, Nakai M, et al. Tumor suppressor miR-22 determines p53-dependent cellular fate through post-transcriptional regulation of p21. Cancer Res. 2011;71(13):4628–39.

38. Jiang X, Hu C, Arnovitz S, Bugno J, Yu M, Zuo Z, et al. miR-22 has a potent anti-tumour role with therapeutic potential in acute myeloid leukaemia. Nat Commun. 2016;7:11452.

39. Song SJ, Ito K, Ala U, Kats L, Webster K, Sun SM, et al. The oncogenic microRNA miR-22 targets the TET2 tumor suppressor to promote hematopoietic stem cell self-renewal and transformation. Cell Stem Cell. 2013;13(1):87–101.

40. Song SJ, Poliseno L, Song MS, Ala U, Webster K, Ng C, et al. MicroRNA-antagonism regulates breast cancer stemness and metastasis via TET-family-dependent chromatin remodeling. Cell. 2013;154(2):311–24.

41. Huang Z-P, Chen J, Seok HY, Zhang Z, Kataoka M, Hu X, et al. MicroRNA-22 regulates cardiac hypertrophy and remodeling in response to stress. Circ Res. 2013;112(9):1234–43.

42. Zhao H, Wen G, Wen G, Huang Y, Yu X, Chen Q, et al. MicroRNA-22 regulates smooth muscle cell differentiation from stem cells by targeting methyl CpG-binding protein 2. Arterioscler Thromb Vasc Biol. 2015;35(4):918–29.

43. Tapscott SJ, Thayer MJ, Weintraub H. Deficiency in rhabdomyosarcomas of a factor required for MyoD activity and myogenesis. Science. 1993;259(5100):1450–3.

44. de la Serna IL, Roy K, Carlson KA, Imbalzano AN. MyoD can induce cell cycle arrest but not muscle differentiation in the presence of dominant negative SWI/SNF chromatin remodeling enzymes. J Biol Chem. 2001;276(44):41486–91.

45. Wang H, Garzon R, Sun H, Ladner KJ, Singh R, Dahlman J, et al. NF-kappaB-YY1-miR-29 regulatory circuitry in skeletal myogenesis and rhabdomyosarcoma. Cancer Cell. 2008;14(5):369–81.

46. Yan D, Dong XDE, Chen X, Wang L, Lu C, Wang J, et al. MicroRNA-1/206 targets c-Met and inhibits rhabdomyosarcoma development. J Biol Chem. 2009;284(43):29596–604.

47. Rao PK, Missiaglia E, Shields L, Hyde G, Yuan B, Shepherd CJ, et al. Distinct roles for miR-1 and miR-133a in the proliferation and differentiation of rhabdomyosarcoma cells. FASEB J. 2010;24(9):3427–37.

48. Balkhi MY, Balkhi MY, Iwenofu OH, Bakkar N, Ladner KJ, Chandler DS, et al. miR-29 acts as a decoy in sarcomas to protect the tumor suppressor A20 mRNA from degradation by HuR. Sci Signal. 2013;6(286):ra63.

49. Diao Y, Guo X, Jiang L, Wang G, Zhang C, Wan J, et al. miR-203, a tumor suppressor frequently down-regulated by promoter hypermethylation in rhabdomyosarcoma. J Biol Chem. 2014;289(1):529–39.

50. Vella S, Pomella S, Leoncini PP, Colletti M, Conti B, Marquez VE, et al. MicroRNA-101 is repressed by EZH2 and its restoration inhibits tumorigenic features in embryonal rhabdomyosarcoma. Clin Epigenetics. 2015;7(1):82.

Figure Legends

Figure 1.

miR-22 and -378 are downregulated in RMS but are induced during myogenic differentiation. A, section of the expression dendrogram including the top 8 differentially expressed miRNAs in human skeletal muscles compared to RMS cells and tissues. Yellow indicates increased expression; black indicates reduced expression. B, Northern blot analysis on total RNA obtained from one muscle and one RMS sample. C and D, real-time PCR analysis in murine satellite cells (C) and C2C12 cells (D) grown in proliferation 'P' or differentiation medium 'D'. E and F, real-time PCR analysis in inducible miR-206-expressing RD18 (NpBI-206) cells (E) and MyoD-expressing NIH 10T½ (NpBI-MyoD) cells (F) (induced, IND; non-induced, NI). Error bars, SD.

Figure 2.

miR-22 interferes with the transforming abilities of RMS cells. A and B, proliferation analysis of inducible miR-22-expressing RD18 (A) and RH30 (B) NpBI-22 cells (induced, IND; non-induced, NI). C and D, cell cycle distribution of RD18 (C) and RH30 (D) NpBI-22 cells (induced, IND; non-induced, NI). E and F, apoptosis assessment of RD18 (E) and RH30 (F) NpBI-22 cells (induced, IND; non-induced, NI). G, Western blot analysis in RD18 and RH30 NpBI-22 cells (induced, IND; non-induced, NI). H and I, quantification and representative images of soft-agar growth of RD18 (H) and RH30 (I) NpBI-22 cells (induced,

IND; non-induced, NI). J and K, invasiveness assessment of RD18 (J) and RH30 (K) NpBI-22 cells (induced, IND; non-induced, NI). Error bars, SEM. *P<0.05; **P<0.01; ***P<0.001 (*t* test).

Figure 3.

miR-22 is transcriptionally regulated by MyoD. A, schematic representation of miR-22 promoter region. The putative binding sites for MyoD are indicated by black boxes. B and C, ChIP analysis of miR-22 promoter regions in NIH NpBI-MyoD cells (induced, IND; non-induced, NI). Two independent oligo pairs were used for miR-22 promoter amplification (oligos A and oligos B). *MCK* and *IgH* enhancers were used as positive and negative controls respectively. Recruitment was relative to normal rabbit IgG. D, dual luciferase assay in NIH NpBI-MyoD cells (induced, IND; non-induced, NI) transfected with the indicated luciferase reporter constructs. Error bars, SD. *P<0.05; **P<0.01; ***P<0.001 (*t* test).

Figure 4.

miR-22 blocks RMS tumor growth and dissemination. A and B, tumor growth curve in nude mice subcutaneously injected with RD18 NpBI-22 cells. In A, half of the mice (*n*=6) were given doxycycline starting at the time of injection (induced, IND), while the rest remained untreated (non-induced, NI). In B, doxycycline was given to half of the mice (*n*=6) only when tumors become palpable (black arrow). C, immunohistochemical analysis of tumors recovered at the end of the treatment explained in B. D and E, Representative images of

whole mount lungs (D, upper panels) and kidneys (E, upper panels) recovered 3 months after tail vein injection of RD18 NpBI-22 cells in nude mice (induced, IND; non-induced, NI). Lower panels show immunohistochemical analysis on sections from the tissues described above. Error bars, SEM.

Figure 5.

TACC1 promotes RMS cell proliferation, anchorage-independent growth and protects RMS cells from apoptosis. A, Western blot analysis in RD18 and RH30 cells expressing the shRNA control (shCTRL) or *TACC1*-directed shRNA (shTACC1). B and C, proliferation analysis of RD18 (B) and RH30 (C) cells described in A. D, Apoptosis assessment of RD18 and RH30 cells described in A. E, quantification and representative images of soft-agar growth of RD18 and RH30 cells described in A after 2 weeks in culture. F, Western blot analysis in RD18 and RH30 cells described in A. G, Western blot analysis in RD18 NpBI-22 cells expressing GFP (CTRL) or TACC1. H, quantification and representative images of soft-agar growth of RD18 NpBI-22 cells described in G and treated with doxycycline (induced, IND) for 2 weeks. Error bars, SEM. *P<0.05; **P<0.01; ***P<0.001 (*t* test).

Figure 6.

RAB5B controls RMS cell migration. A and B, real-time PCR analysis of *RAB5* paralog transcripts in RD18 (A) and RH30 (B) cells. C, Western blot analysis in RD18 cells transfected with siRNA control (siCTRL) or with *RAB5*-directed

siRNAs (siRAB5A, B or C). D and E, representative images (D) and quantification (E) of wound closure of RD18 cells transfected with siCTRL or siRAB5B. F, Western blot analysis in RD18 NpBI-22 cells expressing GFP (CTRL) or RAB5B. G and H, representative images (G) and quantification (H) of wound closure of RD18 NpBI-22 cells maintained in presence of doxycycline (induced, IND) and expressing GFP (CTRL) or RAB5B. Error bars, SEM. *P<0.05 (*t* test).

Figure 7.

miR-22 intercepting ERBB3 counteracts the resistance to MEK inhibitors. A, Proliferation analysis of RD18 NpBI-22 cells induced (IND) or non-induced (NI) and treated with Selumetinib (SEL) or combination. B, Western blot analysis in RD18 NpBI-22 cells induced (IND) or non-induced (NI) and treated with Lapatinib (LAP), Selumetinib (SEL) or combinations for three days. C, quantification and representative images of soft-agar growth of RD18 NpBI-22 cells described in B. D, Dual luciferase assay in 293T cells transfected with the indicated luciferase reporter constructs (wild type, WT; mutated, MUT) along with miR-22. Error bars, SEM. *P<0.05; **P<0.01; ***P<0.001 (*t* test).

Figure 1

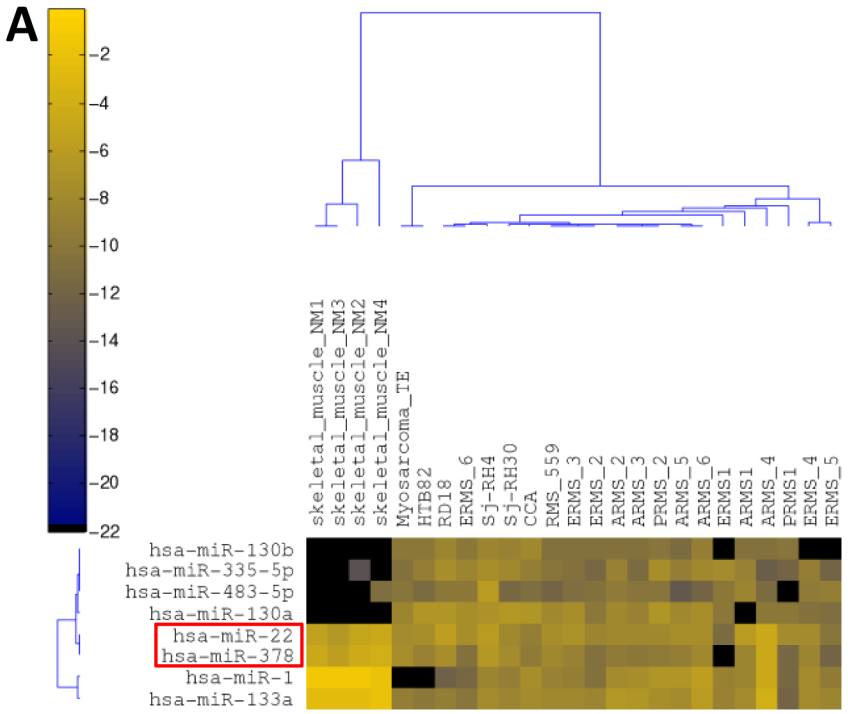
A
skeletal_muscle_NM1
skeletal_muscle_NM3
skeletal_muscle_NM2
skeletal_muscle_NM4
Myosarcoma_TE
HTB82
RD18
ERMS_6
Sj-RH4
Sj-RH30
CCA
RMS_559
ERMS_3
ERMS_2
ERMS_2
ARMS_2
ARMS_3
PRMS_2
ARMS_5
ARMS_6
ERMS1
ARMS1
ARMS_4
PRMS1
ERMS_4
ERMS_5
hsa-miR-130b
hsa-miR-335-5p
hsa-miR-483-5p
hsa-miR-130a
hsa-miR-22
hsa-miR-378
hsa-miR-1
hsa-miR-133a

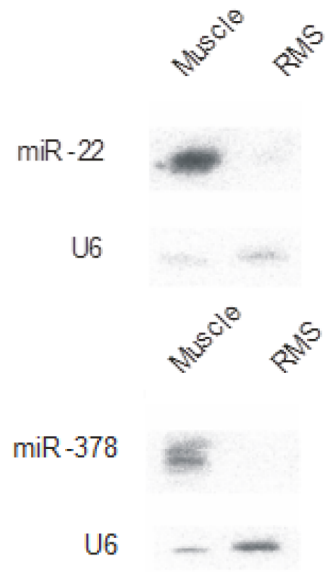
B
Muscle
RMS
miR-22
U6
Muscle
RMS
miR-378
U6

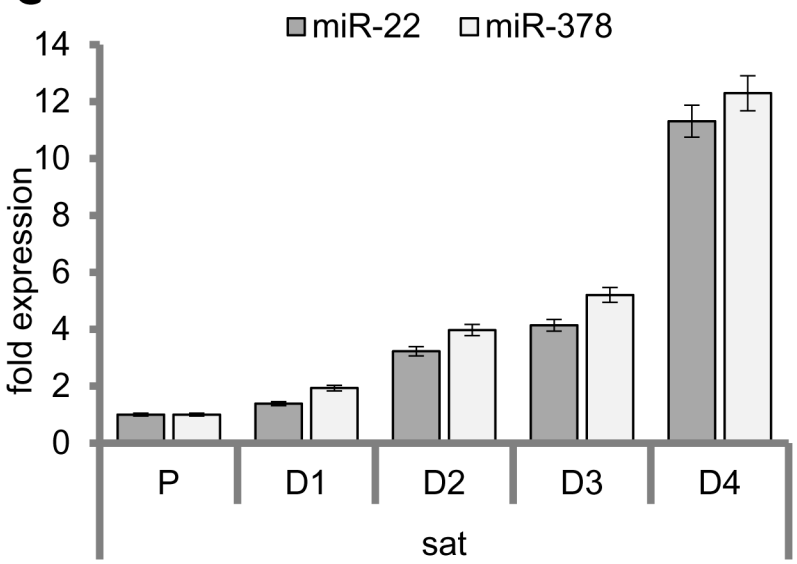
C
miR-22
miR-378
fold expression
P
D1
D2
D3
D4
sat

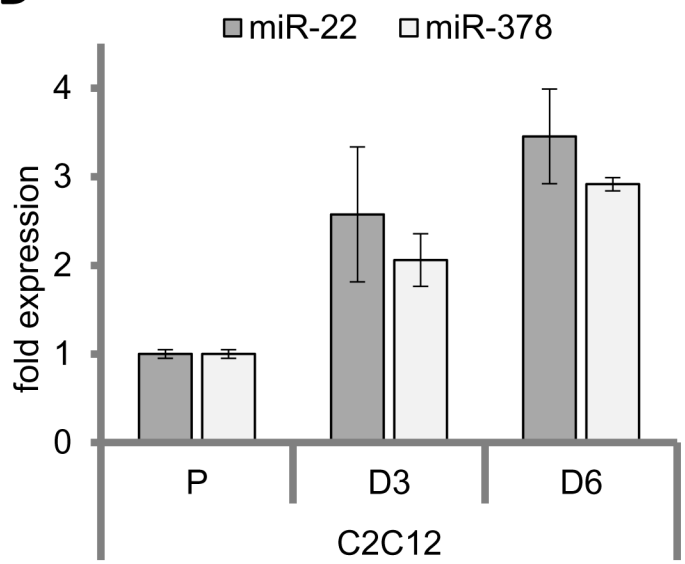
D
miR-22
miR-378
fold expression
P
D3
D6
C2C12

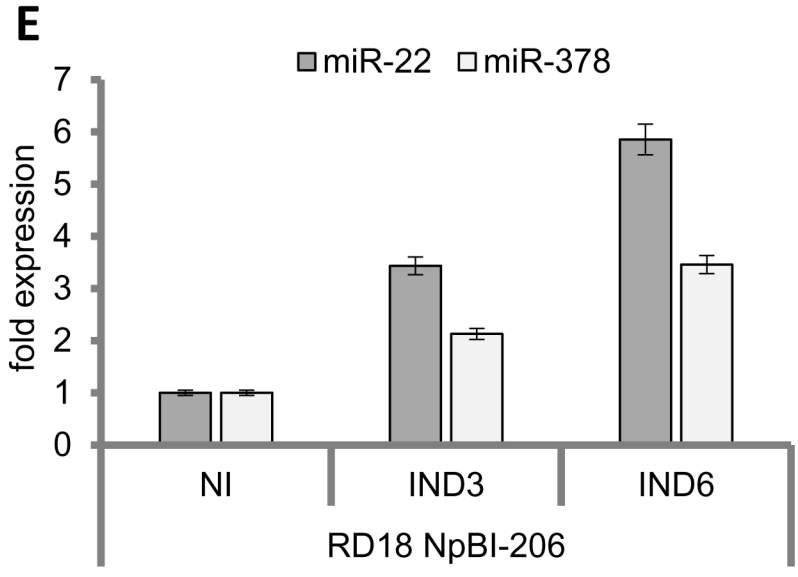
E
miR-22
miR-378
fold expression
NI
IND3
IND6
RD18 NpBI-206

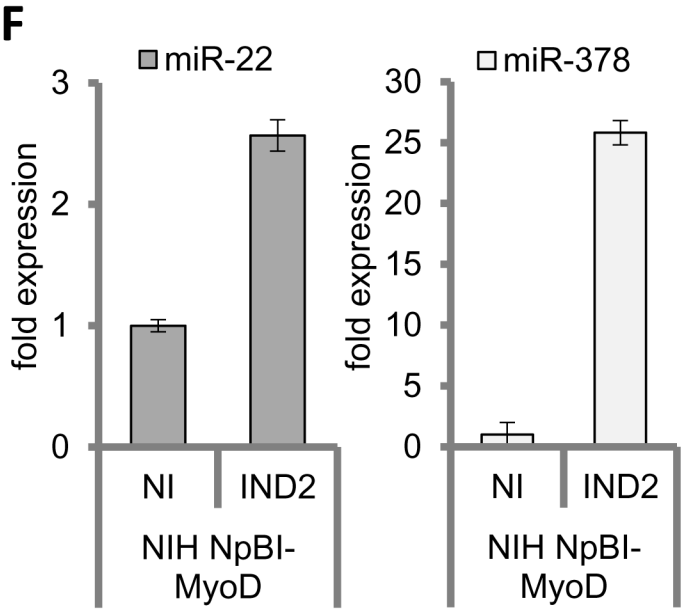
F
miR-22
fold expression
NI
IND2
NIH NpBI-MyoD
miR-378
fold expression
NI
IND2
NIH NpBI-MyoD

Figure 2

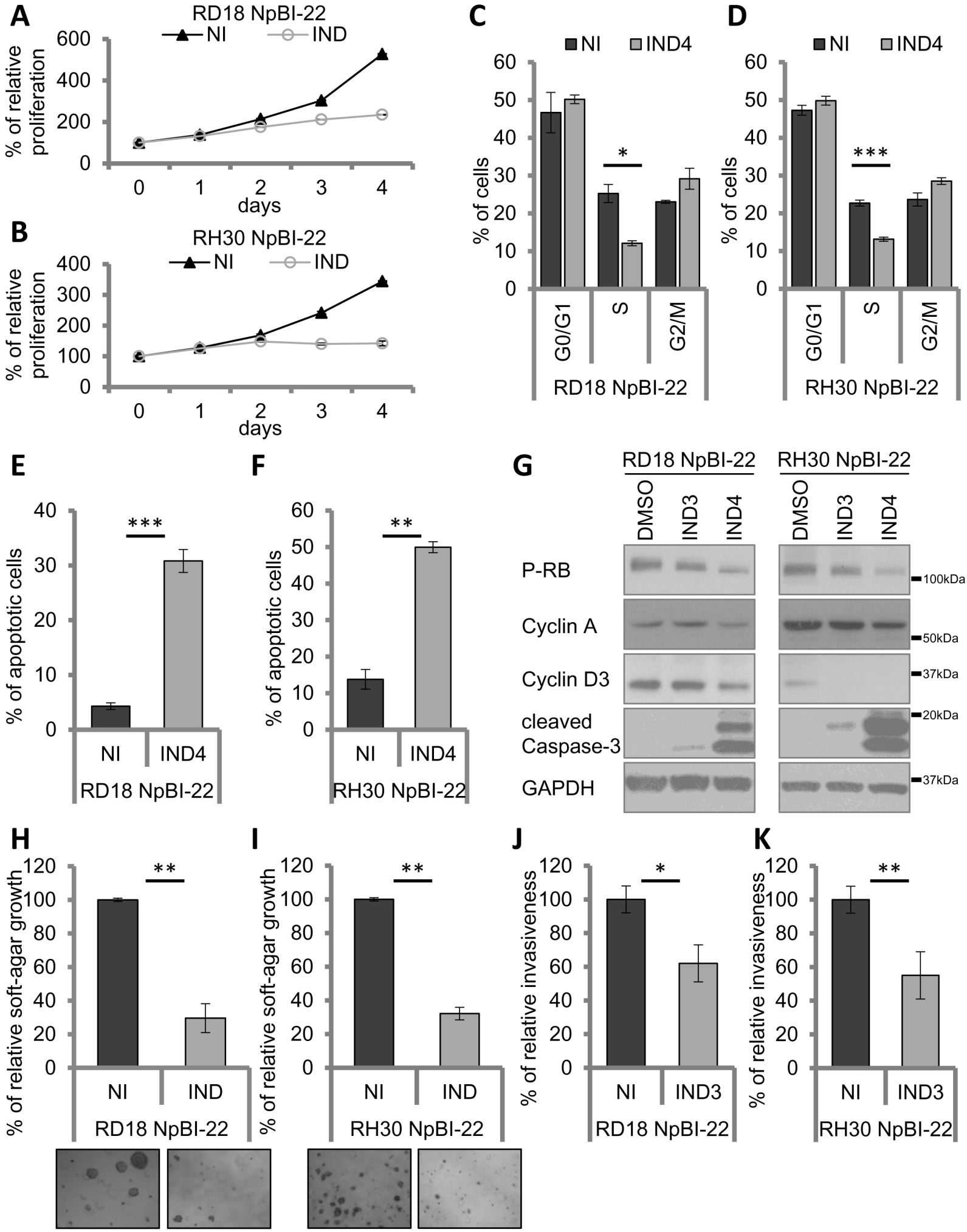
A
RD18 NpBI-22
NI
IND
% of relative proliferation
days
B
RH30 NpBI-22
C
IND4
% of cells
G0/G1
S
G2/M
D
E
% of apoptotic cells
F
G
DMSO
IND3
P-RB
Cyclin A
Cyclin D3
cleaved Caspase-3
GAPDH
100kDa
50kDa
37kDa
20kDa
H
% of relative soft-agar growth
I
J
% of relative invasiveness
K

Figure 3

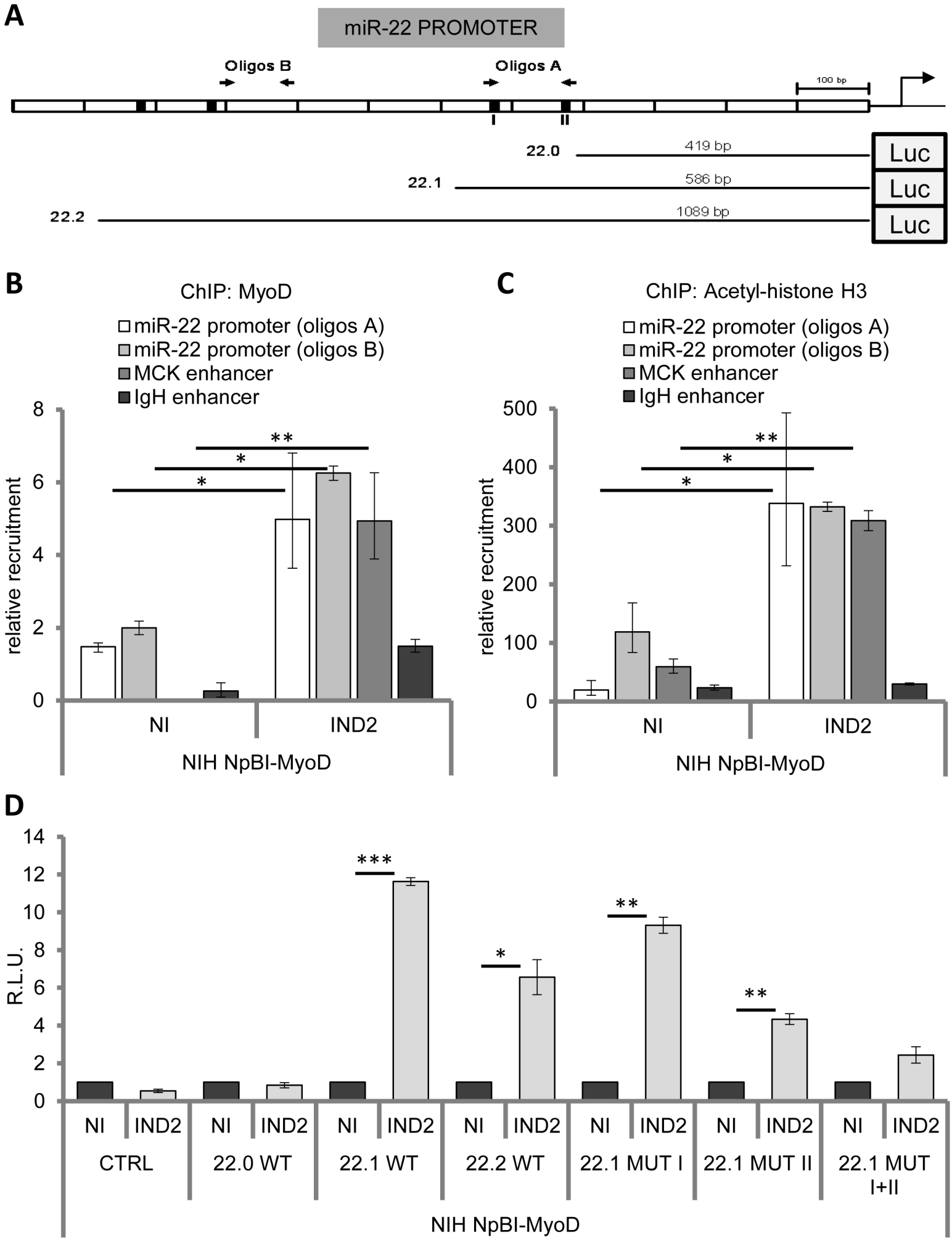
A
miR-22 PROMOTER
Oligos B
Oligos A
100 bp
I
II
22.0
419 bp
Luc
22.1
586 bp
Luc
22.2
1089 bp
Luc
B
ChIP: MyoD
miR-22 promoter (oligos A)
miR-22 promoter (oligos B)
MCK enhancer
IgH enhancer
relative recruitment
0
2
4
6
8
*
*
**
NI
IND2
NIH NpBI-MyoD
C
ChIP: Acetyl-histone H3
miR-22 promoter (oligos A)
miR-22 promoter (oligos B)
MCK enhancer
IgH enhancer
relative recruitment
0
100
200
300
400
500
*
*
**
NI
IND2
NIH NpBI-MyoD
D
R.L.U.
0
2
4
6
8
10
12
14
***
*
**
**
NI
IND2
CTRL
22.0 WT
22.1 WT
22.2 WT
22.1 MUT I
22.1 MUT II
22.1 MUT I+II
NIH NpBI-MyoD

Figure 4

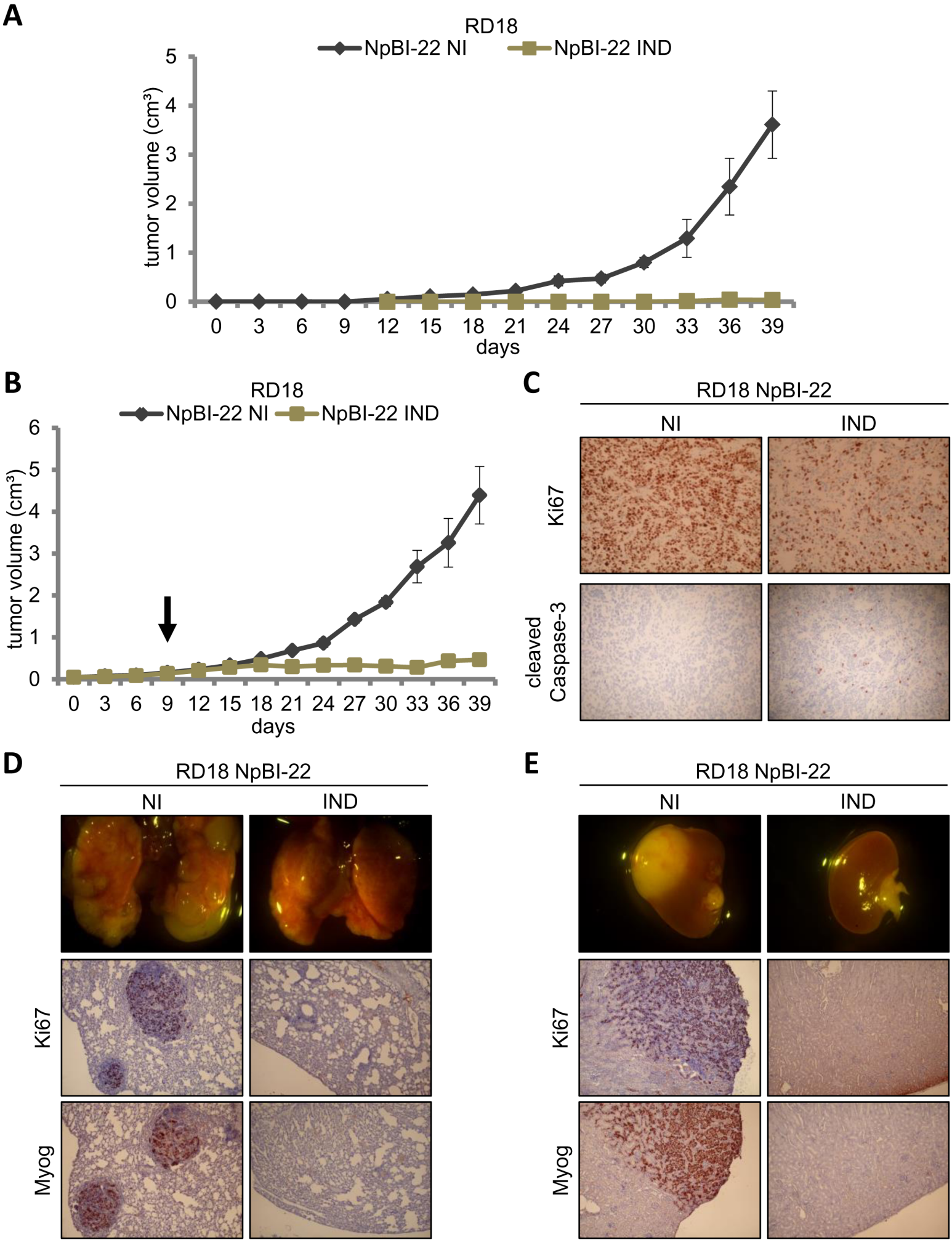
A
RD18
NpBI-22 NI
NpBI-22 IND
tumor volume (cm³)
0
1
2
3
4
5
0 3 6 9 12 15 18 21 24 27 30 33 36 39
days
B
RD18
NpBI-22 NI
NpBI-22 IND
tumor volume (cm³)
0
1
2
3
4
5
6
0 3 6 9 12 15 18 21 24 27 30 33 36 39
days
C
RD18 NpBI-22
NI
IND
Ki67
cleaved Caspase-3
D
RD18 NpBI-22
NI
IND
Ki67
Myog
E
RD18 NpBI-22
NI
IND
Ki67
Myog

Figure 5

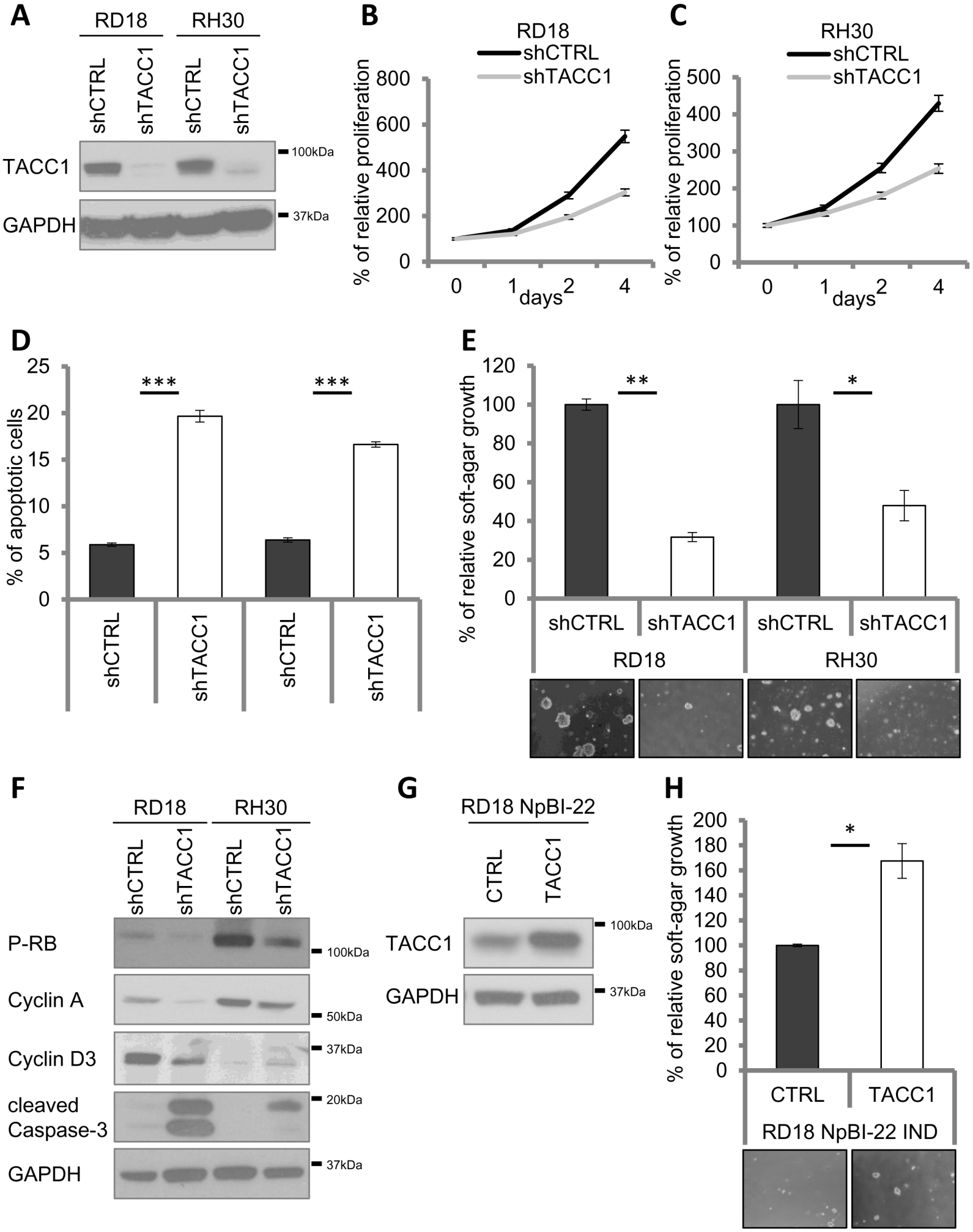
A
RD18
RH30
shCTRL
shTACC1
shCTRL
shTACC1
TACC1
100kDa
GAPDH
37kDa
B
RD18
shCTRL
shTACC1
% of relative proliferation
800
600
400
200
0
0
1
days
2
4
C
RH30
shCTRL
shTACC1
% of relative proliferation
500
400
300
200
100
0
0
1
days
2
4
D
% of apoptotic cells
25
20
15
10
5
0
***
***
shCTRL
shTACC1
shCTRL
shTACC1
E
% of relative soft-agar growth
120
100
80
60
40
20
0
**
*
shCTRL
shTACC1
shCTRL
shTACC1
RD18
RH30
F
RD18
RH30
shCTRL
shTACC1
shCTRL
shTACC1
P-RB
100kDa
Cyclin A
50kDa
Cyclin D3
37kDa
cleaved
Caspase-3
20kDa
GAPDH
37kDa
G
RD18 NpBI-22
CTRL
TACC1
TACC1
100kDa
GAPDH
37kDa
H
% of relative soft-agar growth
200
180
160
140
120
100
80
60
40
20
0
*
CTRL
TACC1
RD18 NpBI-22 IND

Figure 6

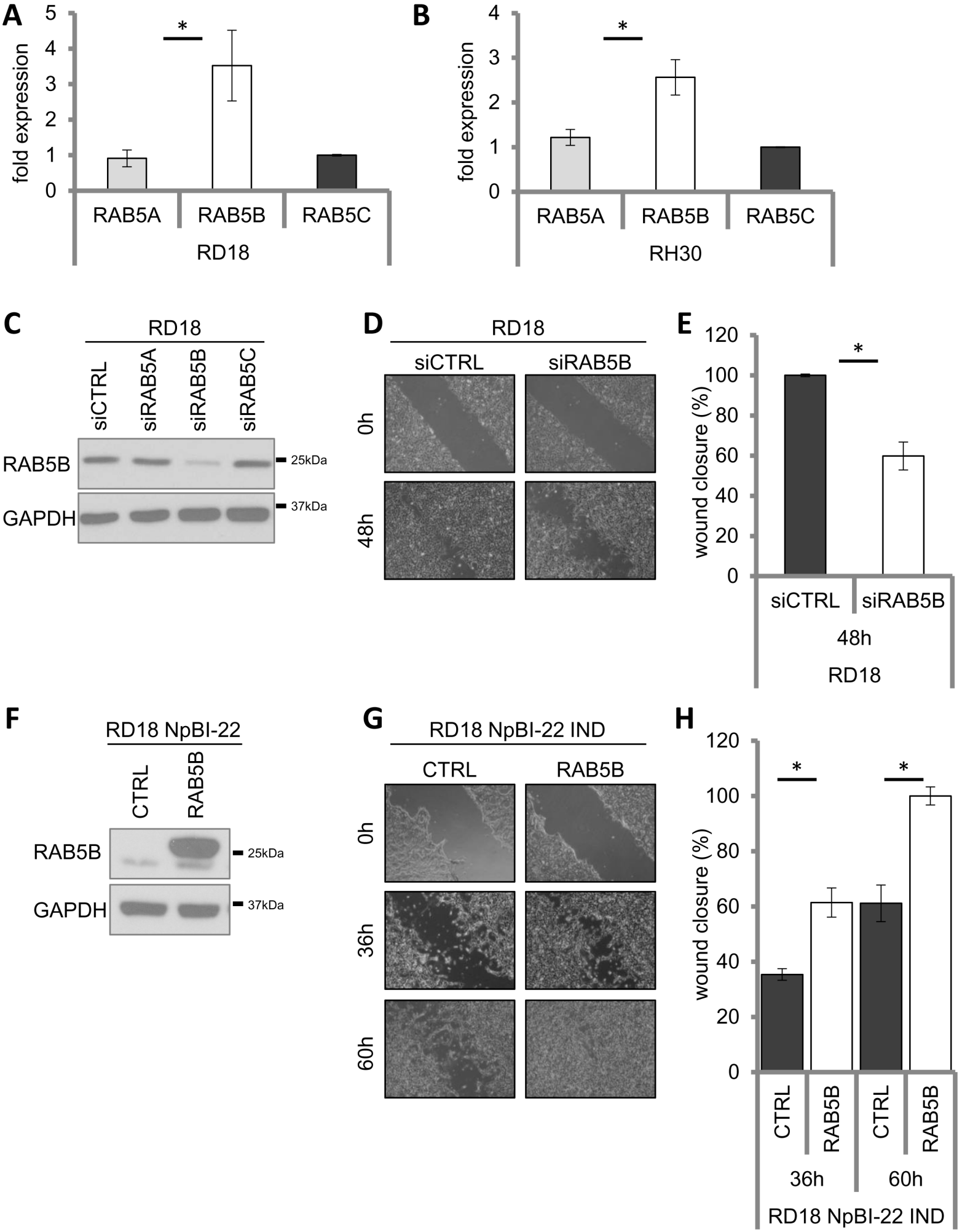
A
fold expression
5
4
3
2
1
0
*
RAB5A
RAB5B
RAB5C
RD18
B
fold expression
4
3
2
1
0
*
RAB5A
RAB5B
RAB5C
RH30
C
RD18
siCTRL
siRAB5A
siRAB5B
siRAB5C
RAB5B
25kDa
GAPDH
37kDa
D
RD18
siCTRL
siRAB5B
0h
48h
E
wound closure (%)
120
100
80
60
40
20
0
*
siCTRL
siRAB5B
48h
RD18
F
RD18 NpBI-22
CTRL
RAB5B
RAB5B
25kDa
GAPDH
37kDa
G
RD18 NpBI-22 IND
CTRL
RAB5B
0h
36h
60h
H
wound closure (%)
120
100
80
60
40
20
0
*
*
CTRL
RAB5B
CTRL
RAB5B
36h
60h
RD18 NpBI-22 IND

Figure 7

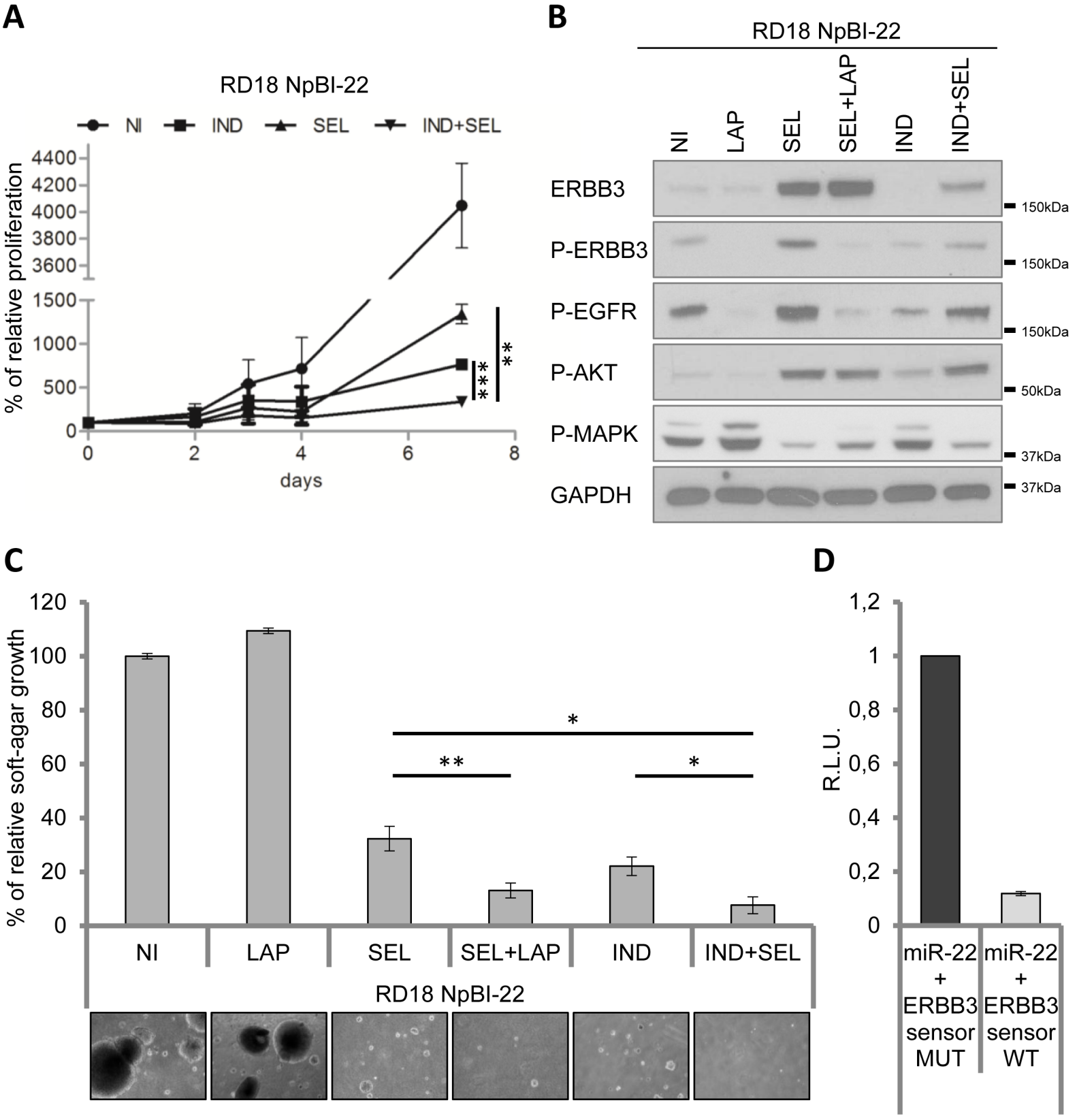
A
RD18 NpBI-22
NI
IND
SEL
IND+SEL
% of relative proliferation
4400
4200
4000
3800
3600
1500
1000
500
0
0
2
4
6
8
days
**
***
**
B
RD18 NpBI-22
NI
LAP
SEL
SEL+LAP
IND
IND+SEL
ERBB3
P-ERBB3
P-EGFR
P-AKT
P-MAPK
GAPDH
150kDa
150kDa
150kDa
50kDa
37kDa
37kDa
C
% of relative soft-agar growth
120
100
80
60
40
20
0
*
**
*
NI
LAP
SEL
SEL+LAP
IND
IND+SEL
RD18 NpBI-22
D
R.L.U.
1,2
1
0,8
0,6
0,4
0,2
0
miR-22 + ERBB3 sensor MUT
miR-22 + ERBB3 sensor WT